Available online at www.sciencedirect.com
ScienceDirect
Scripta Materialia 56 (2007) 589–592
Scripta MATERIALIA
www.actamat-journals.com

Annealing effect on martensitic transformation of severely cold-rolled $Ti_{50}Ni_{40}Cu_{10}$ shape memory alloy

K.N. Lin and S.K. Wu*

Department of Materials Science and Engineering, National Taiwan University, Taipei 106, Taiwan

Received 27 September 2006; revised 18 December 2006; accepted 19 December 2006
Available online 11 January 2007

The annealing effect on the recovery of B2 → B19 and B19 → B19′ transformations of 40% cold-rolled $Ti_{50}Ni_{40}Cu_{10}$ is studied by the differential scanning calorimetry (DSC) and dynamic mechanical analyzer (DMA) tests. The DSC test is only sensitive for measuring the recovery of B2 → B19 transformation, while the DMA test is suitable for both transformations. The change of internal friction values of these two transformations affected by annealing is due mainly to the difference in the rate of change of the transformation volume between them, which is related to their different recovery behaviors and microstructures.

Keywords: Annealing; Cold working; Differential scanning calorimetry (DSC); Shape memory alloys (SMA); Dynamic mechanical analyzer (DMA)

$Ti_{50}Ni_{50-x}Cu_x$ shape memory alloys (SMAs), with $x \leqslant 30$ at.%, have been investigated extensively from various aspects, such as the shape memory effect [1–3], martensitic transformation behavior [4–7], mechanical characteristics [8–10], microstructures [11–16] and internal friction (IF) [17–20]. The transformation sequences of $Ti_{50}Ni_{50-x}Cu_x$ SMAs are B2 ↔ B19′, B2 ↔ B19 ↔ B19′ and B2 ↔ B19 for $x < 5$, $5 \leqslant x \leqslant 20$ and $x > 20$ at.%, respectively [21–24]. Here B2 is parent austenite, and B19 and B19′ are orthorhombic and monoclinic martensite, respectively.

Traditionally, differential scanning calorimetry (DSC) has been employed to investigate martensitic transformation behavior of SMAs. Lo et al. [17] and Ren et al. [25] showed that the transformation shear strain required in B2 ↔ B19 transformation (~8%) of $Ti_{50}Ni_{40}Cu_{10}$ is larger than that in B19 ↔ B19′ (~2%). Thus, the transformation enthalpy, ΔH, of B2 ↔ B19 transformation is significantly larger than that of B19 ↔ B19′ transformation and the DSC technique is suitable for investigating B2 ↔ B19 transformation [17]. Dynamic mechanical analyzer (DMA) is another technique for investigating martensitic transformation of SMAs. DMA measurement indicates that $Ti_{50}Ni_{40}Cu_{10}$ exhibits two significant IF peaks corresponding to B2 ↔ B19 and B19 ↔ B19′ transformations [17–20]. Thus, DMA is useful for investigating both B2 ↔ B19 and B19 ↔ B19′ transformations.

A cold-working process can generate high-density defects, large residual stresses and distortion in cold-worked alloys. These imperfections greatly affect martensitic transformation behavior and can be reduced or released by annealing treatment. However, it is unclear which between B2 → B19 and B19 → B19′ transformations will recover first after annealing treatment for cold-worked $Ti_{50}Ni_{40}Cu_{10}$ SMA. In this study, the annealing effect on B2 → B19 and B19 → B19′ transformations of 40% cold-rolled $Ti_{50}Ni_{40}Cu_{10}$ is investigated by DSC and DMA. The different recovery behaviors of B2 → B19 and B19 → B19′ transformations under different annealing conditions are also discussed.

$Ti_{50}Ni_{40}Cu_{10}$ ingot was prepared by vacuum arc-remelting (VAR) method in which high-purity Ti (99.8 wt.%), Ni (99.9 wt.%) and Cu (99.99 wt.%) were remelted six times in a high-purity Ar atmosphere. The ingot was hot-rolled at 900 °C to a plate of 2 mm thickness, solution-treated at 900 °C for 1 h and subsequently quenched into water. The oxidation layer of the plate was chemical etched by a solution composed of HF:HNO_3:H_2O in a 1:5:20 volume ratio. After removing the oxidation layer, the thickness of the plate became 1.9 mm, and the plate was cut into 90 mm × 20 mm strips with the longitude along the hot-rolling direction. Thereafter, the strips were cold-rolled along the hot-rolling direction to 1.15 mm at room temperature. The total reduction in thickness was about 40%. After

* Corresponding author. Tel.: +886 2 2363 7846; fax: +886 2 2363 4562; e-mail: skw@ntu.edu.tw

1359-6462/$ - see front matter © 2007 Acta Materialia Inc. Published by Elsevier Ltd. All rights reserved.
doi:10.1016/j.scriptamat.2006.12.016

cold-rolling, the strips were cut into 40 mm × 4.5 mm specimens, sealed in evacuated quartz tubes and then annealed at 500 and 650 °C for different time intervals. Transformation temperature and enthalpy of cold-rolled and annealed specimens were determined by TA Q10 DSC equipment with 10 °C min^{-1} cooling/heating rate. The IF peaks and their tan δ values of cold-rolled and annealed specimens were determined by TA 2980 DMA equipment with 3 °C min^{-1} cooling/heating rate under constant frequency (1 Hz) and amplitude (2 μm, with a strain of 2×10^{-5}). The testing temperature range was from +150 to −150 °C in both DSC and DMA tests. The abbreviations "tan δ_1" and "tan δ_2" are employed to represent the IF peak values of B2 → B19 and B19 → B19′ transformations, respectively.

Figures 1 and 2 show the DSC results of 40% cold-rolled $Ti_{50}Ni_{40}Cu_{10}$ specimens annealed at 500 and 650 °C, respectively, for different time intervals. The annealing conditions for Figure 1a–c are 500 °C for 1, 24 and 96 h, respectively, and those for Figure 2a–c are 650 °C for 0.5, 24 and 72 h, respectively. After annealing at 500 °C for 1 h, as shown in Figure 1a, the B2 → B19 transformation peak clearly recovers while the B19 → B19′ transformation peak is insignificant. After further annealing, as shown in Figure 1b, the B2 → B19 transformation peak becomes sharper and the B19 → B19′ transformation peak appears but is still not clear. Finally, after annealing for 500 °C at 96 h, as shown in Figure 1c, both B2 → B19 and B19 → B19′ transformation peaks become clear. Under 650 °C annealing, both B2 → B19 and B19 → B19′ transformation peaks recover obviously within 0.5 h, as shown in Figure 2a. Figure 3 plots the relationship of ΔH_c versus annealing time for the specimens of Figures 1 and 2, annealed at 500 and 650 °C, respectively. Here ΔH_c is the transformation enthalpy of the DSC cooling curve.

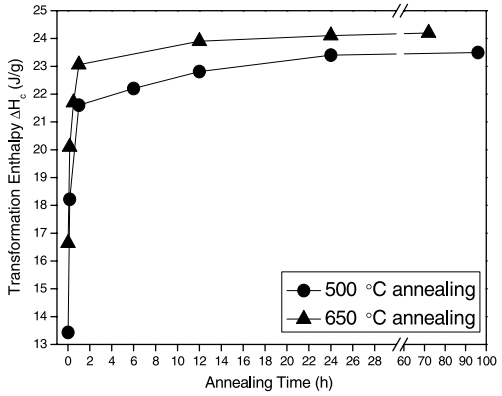

Figure 3. The relationship of ΔH_c versus annealing time interval under 500 and 650 °C annealing.

Figure 3 shows that the ΔH_c value increases obviously within 1 h and then becomes saturated when the annealing time is prolonged to about 23.5 J g^{-1} under 500 and 650 °C annealing.

According to Figure 3, ΔH_c values of specimens annealed at 500 °C for 1 h and 650 °C for 0.5 h, and those at 500 °C for 24 h and 650 °C for 1 h are almost the same (about 21.6 and 23.4 J g^{-1}, respectively). Figure 4a and b shows the DMA results of these two pairs of specimens. It is obvious that, even if the ΔH_c values are approximately equal, the IF peaks of the B2 → B19 (tan δ_1) and B19 → B19′ (tan δ_2) transformations for different annealed $Ti_{50}Ni_{40}Cu_{10}$ specimens are not identical. From Figure 4, for specimens having equal ΔH_c, their tan δ_1 values are almost the same while their tan δ_2 values are quite different. This is because the ΔH_c value is contributed mainly by the B2 → B19 transformation, rather than the B19 → B19′ transformation

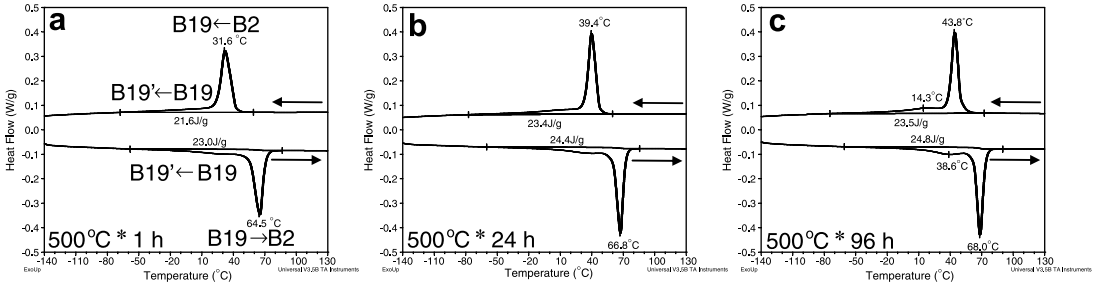

Figure 1. DSC results of 40% cold-rolled $Ti_{50}Ni_{40}Cu_{10}$ specimens annealed at 500 °C. (a) 1 h, (b) 24 h and (c) 96 h.

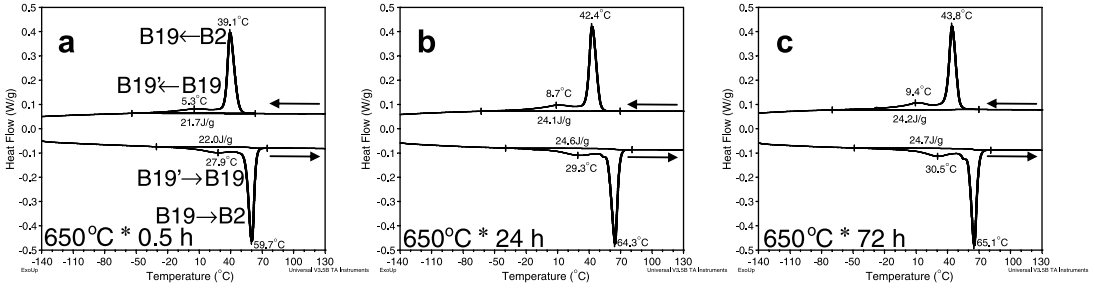

Figure 2. DSC results of 40% cold-rolled $Ti_{50}Ni_{40}Cu_{10}$ specimens annealed at 650 °C. (a) 0.5 h, (b) 24 h and (c) 72 h.

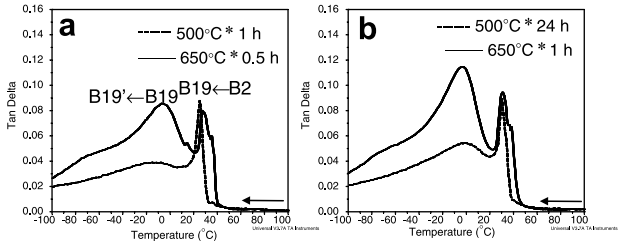

Figure 4. DMA results of cold-rolled and annealed $Ti_{50}Ni_{40}Cu_{10}$ specimens having the same ΔH_c values. (a) Specimens annealed at 500 °C for 1 h and at 650 °C for 0.5 h, and (b) specimens annealed at 500 °C for 24 h and at 650 °C for 1 h.

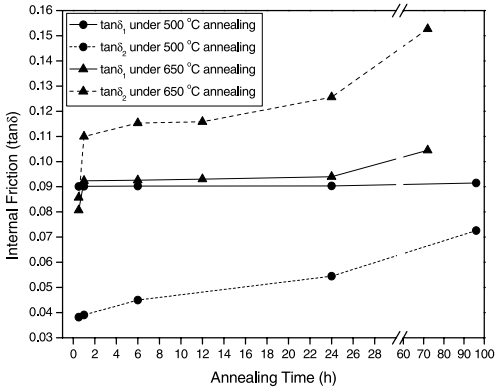

Figure 6. The relationship of $\tan\delta_1$ and $\tan\delta_2$ versus annealing time interval under 500 and 650 °C annealing.

[17]. In other words, the annealing effect on cold-rolled $Ti_{50}Ni_{40}Cu_{10}$ specimens is not sensitive for the recovery of the B19 → B19′ transformation, as indicated by the DSC results.

The DMA results of 40% cold-rolled and annealed $Ti_{50}Ni_{40}Cu_{10}$ specimens are shown in Figures 4 and 5. After annealing at 500 °C for 1 h, as shown in Figure 4a, the B2 → B19 transformation peak recovers obviously while the B19 → B19′ transformation peak is not so clear. After further annealing, as shown in Figures 4b and 5a, the B19 → B19′ transformation peak gradually becomes apparent but the change in the height of the B2 → B19 transformation peak can be negligible. Under 650 °C annealing, both the B2 → B19 and B19 → B19′ transformation peaks recover obviously within 0.5 h annealing, as shown in Figure 4a. After further annealing, as shown in Figures 4b and 5b and c, $\tan\delta_2$ grows rapidly while $\tan\delta_1$ grows only a little. From Figures 4 and 5, $\tan\delta_1$ and $\tan\delta_2$ versus annealing time under 500 and 650 °C annealing are plotted in Figure 6. It is obvious that B2 → B19 transformation recovers rapidly at first and $\tan\delta_1$ is saturated to about 0.09–0.1 under both 500 and 650 °C annealing. However, the recovery of B19 → B19′ transformation shows quite different behavior. Under 650 °C annealing, $\tan\delta_2$ grows rapidly and is always larger than $\tan\delta_1$, while under 500 °C annealing, $\tan\delta_2$ grows slowly and is always smaller than $\tan\delta_1$.

Zu et al. [26] investigated the recrystallization behavior of heavy ion-irradiation-induced amorphized $Ti_{50}Ni_{43}Cu_7$ SMA by in situ transmission electron microscopic observation. They pointed out that the recrystallization of amorphized $Ti_{50}Ni_{43}Cu_7$ started at 273 °C. Tsuji and Nomura [27] investigated the relationship between hardness and annealing temperature of 27% cold-rolled $Ti_{50.5}Ni_{40.5}Cu_9$ SMA annealed at 450, 500, 550, 600 and 750 °C for 1 h. They suggested that annealing temperature up to 500 °C allows 27% cold-rolled $Ti_{50.5}Ni_{40.5}Cu_9$ to recover, and that higher annealing temperatures can rapidly remove the internal defects and distortion, and further cause recrystallization and grain growth. According to these reports, we propose that the recrystallization temperature of 40% cold-rolled $Ti_{50}Ni_{40}Cu_{10}$ is lower but close to 500 °C. Therefore, only recrystallization occurs under 500 °C annealing, whereas both recrystallization and grain growth occur rapidly under 650 °C annealing.

The aforementioned results indicate that different recovery behaviors of B2 → B19 and B19 → B19′ transformations exhibit in between ΔH_c and IF resulted from different testing methods of DSC and DMA measurements. In the DSC test, the driving force of transformation is attributed only to the change in temperature, and the ΔH_c value can be employed to estimate the total transformation volume. In the DMA test, the driving force of transformation comes not only from the temperature change but also from the applied stress. The IF of a first-order phase transformation can be predicted by the De Jonghe–Delorme model [28,29]:

$$\tan\delta \propto \frac{1}{\omega}\frac{\mathrm{d}\Psi(V_m)}{\mathrm{d}V_m}\left(\frac{\partial V_m}{\partial T}\frac{\partial T}{\partial t}+\frac{\partial V_m}{\partial \sigma}\frac{\partial \sigma}{\partial t}\right) \quad (1)$$

where ω is the angular frequency of applied stress, V_m is the volume fraction of martensite, $\Psi(V_m)$ is a monotonous function associated with transformation volume change or shape strain, T is temperature, t is time and σ is the stress that induces martensitic transformation

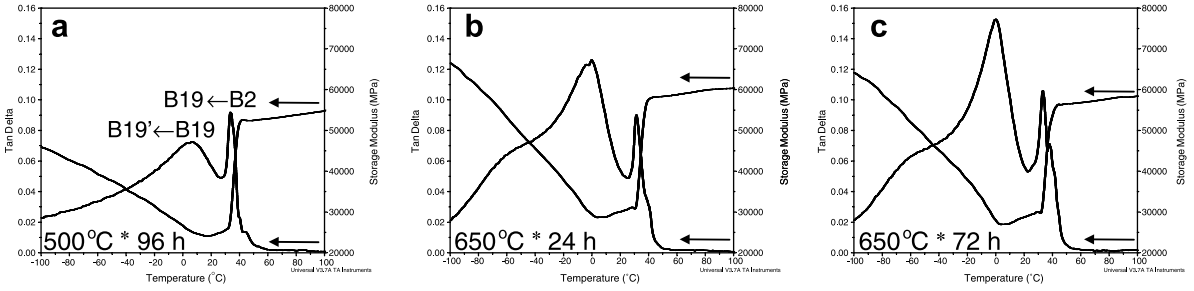

Figure 5. DMA results of 40% cold-rolled and annealed $Ti_{50}Ni_{40}Cu_{10}$ specimens. Annealing at (a) 500 °C for 96 h, (b) 650 °C for 24 h and (c) 650 °C for 96 h.

or reorientation of martensite variants. In this study, ω and the temperature changing rate are kept as constants (1 Hz and 3 °C min^{-1}, respectively), and σ is in the order of 1 MPa, which is not large enough to induce martensitic transformation or to reorient martensite variants. In supposing that $d\Psi(V_m)/dV_m$ is constant for all thermoelastic martensites [30], the De Jonghe–Delorme model can be simplified as

$$\tan\delta \propto \frac{\partial V_m}{\partial T} \tag{2}$$

The $\tan\delta$ value is now simply determined by dV_m/dT, that is, the volume of martensite formation per unit temperature. From Figure 4, ΔH_c and $\tan\delta_1$ of the annealed specimens show almost the same values but their $\tan\delta_2$ values do not. This implies that, for these specimens, their dV_m/dT of the B2 → B19 transformation, $(dV_m/dT)_{B2\rightarrow B19}$, can be regarded as almost equal, but that of the B19 → B19′ transformation, $(dV_m/dT)_{B19\rightarrow B19'}$, cannot be. The different values of $(dV_m/dT)_{B2\rightarrow B19}$ and $(dV_m/dT)_{B19\rightarrow B19'}$ are attributed to the different intrinsic crystal structures associated with B19 and B19′ martensites, that is, defect-free B19 and $(0\,0\,1)_{B19'}$ twinned B19′ martensites [4]. Under 500 °C annealing, only recrystallization occurs, the grain size is small and grain size distribution is not uniform, and thus B19 → B19′ transformation is more suppressed. Under 650 °C annealing, however, both recrystallization and grain growth occur quickly. At this time, $\tan\delta_2$ also increases in the same pace as the annealing recovery because the grain size increases and the grain size distribution becomes more uniform.

The annealing effect on the recovery of B2 → B19 and B19 → B19′ transformations of 40% cold-rolled $Ti_{50}Ni_{40}Cu_{10}$ is investigated by DSC and DMA techniques in this study. Experimental results show that the recovery behaviors of B2 → B19 and B19 → B19′ transformations are different. The DSC and DMA results of annealed specimens having equal ΔH_c value show that the ΔH_c value of the DSC curve is mainly contributed by B2 → B19 transformation and so the test is not sensitive for measuring the recovery of B19 → B19′ transformation. However, the DMA test is useful for investigating both B2 ↔ B19 and B19 ↔ B19′ transformations. The recovery of B2 → B19 transformation can proceed with annealing at 500 °C for 1 h, while that of B19 → B19′ requires annealing at 650 °C for 1 h. The recrystallization temperature of 40% cold-rolled $Ti_{50}Ni_{40}Cu_{10}$ is lower but close to 500 °C. The different recovery behaviors of B2 → B19 and B19 → B19′ transformations are due mainly to the different microstructures of defect-free B19 and $(0\,0\,1)_{B19'}$ twinned B19′ martensites. The IF $\tan\delta$ values of B2 → B19 and B19 → B19′ transformation peaks are proposed to be proportional to dV_m/dT values, which are different for the B2 → B19 and B19 → B19′ transformations. This causes the different recovery behaviors of B2 → B19 and B19 → B19′ transformations.

The authors gratefully acknowledge the financial support from the National Science Council (NSC), Taiwan, Republic of China, under Grant NSC95-2221-E002-163.

[1] T.H. Nam, T. Saburi, Y. Kawamura, K. Shimizu, Mater. Trans., JIM 31 (1990) 262.
[2] T.H. Nam, T. Saburi, K. Shimizu, Mater. Trans., JIM 33 (1992) 814.
[3] H. Sehitoglu, I. Karaman, X. Zhang, A. Viswanath, Y. Chumlyakov, H.J. Maier, Acta Metall. 49 (2001) 3621.
[4] T. Fukuda, T. Saburi, T. Chihara, Y. Tsuzuki, Mater. Trans., JIM 36 (1995) 1244.
[5] T. Fukuda, M. Kitayama, T. Kakeshita, T. Saburi, Mater. Trans., JIM 37 (1996) 1540.
[6] G. Mazzolai, A. Biscarini, B. Coluzzi, F.M. Mazzolai, A.R. Ross, T.A. Lograsso, Mater. Sci. Eng. A 370 (2004) 497.
[7] X. Ren, N. Miura, K. Taniwaki, K. Otsuka, T. Suzuki, K. Tanaka, Yu.I. Chumlyakov, M. Asai, Mater. Sci. Eng. A 273–275 (1999) 190.
[8] K.N. Melton, O. Mercier, Metall. Trans. 9A (1978) 1487.
[9] T. Saburi, T. Takagaki, S. Nenno, K. Koshino, MRS Int. Mtg. Adv. Mats. 9 (1988) 147.
[10] J.L. Proft, K.N. Melton, T.W. Duerig, MRS Int. Mtg. Adv. Mats. 9 (1988) 159.
[11] P.L. Potapov, A.V. Shelyakov, D. Schryvers, Scripta Mater. (2001) 1.
[12] T. Tadaki, K. Shmizu, C.M. Wayman, Mater. Trans., JIM 32 (1991) 43.
[13] R.H. Bricknell, K.N. Melton, O. Mercier, Metall. Trans. 10A (1979) 693.
[14] R.H. Bricknell, K.N. Melton, Metall. Trans. 11A (1980) 1541.
[15] T. Tadaki, C.M. Wayman, Metallography 15 (1982) 233.
[16] T. Tadaki, C.M. Wayman, Metallography 15 (1982) 247.
[17] Y.C. Lo, S.K. Wu, H.E. Horng, Acta Metall. Mater. 41 (1993) 747.
[18] S.K. Wu, H.C. Lin, J. Alloys Compd. 355 (2003) 72.
[19] I. Yoshida, D. Monma, K. Otsuka, M. Asai, H. Tsuzuki, J. Alloys Compd. 355 (2003) 79.
[20] I. Yoshida, D. Monma, K. Iino, K. Otsuka, M. Asai, Mater. Sci. Eng. A 370 (2004) 444.
[21] O. Mercier, K.N. Melton, Metall. Trans. 10A (1979) 387.
[22] H. Miyamato, T. Taniwaki, T. Ohba, K. Otsuka, S. Nishigori, K. Katc, Scripta Mater. 53 (2005) 171.
[23] T.H. Nam, T. Saburi, K. Shimizu, Mater. Trans., JIM 31 (1990) 959.
[24] T.H. Nam, T. Saburi, Y. Nakata, K. Shimizu, Mater. Trans., JIM 31 (1990) 1050.
[25] X. Ren, N. Miura, J. Zhang, K. Otsuka, K. Tanaka, M. Koiwa, T. Suzuki, Yu.I. Chumlyakov, M. Asai, Mater. Sci. Eng. A 312 (2001) 196.
[26] X.T. Zu, S. Zhu, X. Xiang, L.P. You, Y. Huo, L.M. Wang, Mater. Sci. Eng. A 363 (2003) 352.
[27] K. Tsuji, K. Nomura, Scripta Metall. Mater. 24 (1990) 2037.
[28] J.F. Delorme, R. Schmid, M. Robin, P. Gobin, J. Phys. 32 (1971) C2–C101.
[29] W. Dejonghe, R. De Batist, L. Delaey, Scripta Metall. 10 (1976) 1125.
[30] O. Mercier, K.N. Melton, Y. De Préville, Acta Metall. 27 (1979) 1467.